Talanta 267 (2024) 125211

Contents lists available at ScienceDirect

Talanta

journal homepage: www.elsevier.com/locate/talanta

A plasmonic gold nano-surface functionalized with the estrogen receptor for fast and highly sensitive detection of nanoplastics

Mimimorena Seggio [a,1], Francesco Arcadio [b,1], Nunzio Cennamo [b], Luigi Zeni [b,**], Alessandra Maria Bossi [a,*]

[a] University of Verona, Department of Biotechnology, Strada Le Grazie 15, 37134, Verona, Italy
[b] University of Campania Luigi Vanvitelli, Department of Engineering, Via Roma 29, 81031 Aversa, Italy

ARTICLE INFO

Handling Editor: Prof. J.-M. Kauffmann

Keywords:
Nanoplastic
Optical sensors
Nanoplasmonic
Nanogratings
Biosensor
Sea water

ABSTRACT

Nanoplastics are a global emerging environmental problem whose effects might pose potential threats to the human's health. Despite the relevance of the issue, fast, reliable and quantitative *in situ* analytical approaches to determine nanoplastics are not yet available. The aim of this work was to devise an optical sensor with the goal of direct detecting and quantifying nanoplastics in seawater without sample pre-treatments. To this purpose, a nano-plasmonic biosensor was developed by exploiting an Estrogen Receptor (ER) recognition element grafted onto a polymer-based gold nanograting (GNG) plasmonic platform. The ER-GNG biosensor required just minute sample volumes (2 μL), allowed rapid detection (3 min) and enabled to determine nanoplastics in simulated seawater with a linear dynamic concentrations range of 1–100 ng/mL, thus encompassing the expected environmental loads. The nanostructured grating (GNG) provided remarkable performance enhancements, extending the measurement range across five orders of magnitude, thanks to the both the SPR and the localized SPR phenomena occurring at the GNG chip. At last, the ER-GNG biosensor was tested on real seawater samples collected in the Naples area and the results (~30 ng/mL) were verified by a conventional approach (filtration and evaporation), confirming the ER-GNG sensor offers a straightforward and highly sensitive method for the direct in-field nanoplastics monitoring.

1. Introduction

Synthetic polymers are among the most important classes of materials of the 21st century. Since the beginning of the 20th century, polymers, commonly intended as plastics, found widespread industrial and daily-life uses. As a consequence, the plastics production has been steadily increasing every year, globally counting for 368 million tons in 2019 [1,2]. The outcome of such a massive use of plastics is the production of huge amounts of plastic wastes, which unfortunately accumulate in the environment, where the effects of chemical and physical stresses crack the plastics materials into pieces. Plastic fragments are classified according to their size into macro-, meso- (>5 mm), micro- (1 μm–5 mm) and nano-plastics (particles size <1 μm) [3–7].

To date, nanoplastics are probably the least known source of pollution, while potentially one of the most hazardous. Recently, nanoplastics were reported in numerous environmental matrices, including freshwater [8,9] snow [10–12], ice [13–15], soil [16–18], sediment [19–21], terrestrial and aquatic biota [22–25], air [26–30]. The effect of nanoplastics on human health is yet not fully elucidated. The human exposure to nanoplastics might occur *via* oral inhalation, ingestion, or absorption by the skin. According to the current data, nanoplastics are mostly uptaken *via* ingestion of seafood or by drinking contaminated water. The nanometric size increases the nanoplastic's reactivity and the capability to pass through cellular barriers and accumulate inside the organisms [31,32]. Such a behaviour was confirmed in *in vivo* experiments that showed that nanoparticles penetrate the intestinal barrier and can be further translocated into blood vessels [33]. Moreover, numerous studies proved nanoplastics to be the causative agent of toxicity at various levels such as neurological, reproductive, and developmental of the organisms [34–36].

* Corresponding author.
** Corresponding author. Department of Engineering, University of Campania Luigi Vanvitelli, via Roma 29, 81031 Aversa, Italy.
E-mail addresses: mimimorena.seggio@univr.it (M. Seggio), francesco.arcadio@unicampania.it (F. Arcadio), nunzio.cennamo@unicampania.it (N. Cennamo), luigi.zeni@unicampania.it (L. Zeni), alessandramaria.bossi@univr.it (A.M. Bossi).
[1] Shared authorship: Mimimorena Seggio, Francesco Arcadio.

https://doi.org/10.1016/j.talanta.2023.125211
Received 30 May 2023; Received in revised form 10 September 2023; Accepted 14 September 2023
Available online 16 September 2023

The first step towards understanding the impact of nanoplastics on living organisms is to evaluate the relationship between their environmental concentrations and the effects. This has proven to be a tough analytical challenge, due to the lack of validated methods for their quantification and to the inherent difficulties posed by the detection of sub-micrometer fragments [37].

Concerning the quali/quantitative determination of nanoplastics in real samples, to date protocols rely on a pre-concentration step, which increases the number of particles per vol/wt. To this purpose different strategies have been proposed, such as ultrafiltration, ultracentrifugation and solvent evaporation [38] coupled with classical analytical methods [39–41], whereas XPS, FTIR, nano-IR, Raman tweezers spectroscopy [42], HPLC or Py-GC-MS [43–45], were used to chemically identify the material composing the plastic particles.

Recently, the area of bio- and chemosensors started focusing on the quali/quantification of micro- and nano-plastics. Optical sensing based on Surface Plasmon Resonance (SPR) and Localized Surface Plasmon Resonance (LSPR) [46,47] for its label free detection and high sensitivity can offer solutions. Tuoriniemi et al. [48] proposed an easy plasmonic detection for nanoplastics, just based on the refractive index (RI) variations caused by the plastic particles adsorption to the plasmonic metal surface. The system was very straightforward, though completely non-selective and thus prone to false positives. The range of response was 1–80 ppm, thus it was far from the direct determination in real samples. An improved plasmonic sensor-design was proposed by Huang et al. [49]: plastic selectivity was introduced by exploiting the alpha estrogen receptor (ER) as selective element. The ER belongs to the nuclear hormone receptors superfamily, which are ligand-activated transcription factors. Estradiol is the natural ligand of ER and upon its binding the ER activates transcriptional processes and/or signalling events. There are two isoforms of the estrogen receptors, namely ERα and Erβ. In the present work, ERα was chosen as recognition element, according to Ref. [49]. The full-length sequence of ERα is composed of 595 amino acids and has a MW of 67 kDa, while the estimated radius is ~3.6 nm [50]. The ER has been showing ability to interact with microplastic particles, with reported apparent dissociation constants ranging between 0.19 nM and 3.32 nM, depending on the microplastic type and with a dynamic range of response between 0.5 and 6.5 nM [49]. This kind of interaction is mainly hydrophobically driven [49].

In the present work, we aimed at proposing a solution to the detection and quantification of nanoplastics, yet meeting the concentration levels found in the environment. We report the development of a biosensor based on a nanostructured plasmonic optical platform functionalized with the ER receptor. The ER was coupled to a gold nanograting (GNG) structures recently developed and described in Refs. [51,52] in order to attune the plasmonic sensor performance towards concentrations in the real scenario range. To this purpose spherical poly (methyl methacrylate) (PMMA) nanoplastics were used as a model. Indeed, PMMA has undergone a significant production's increment during the Covid-19 pandemic, for the Plexiglass separation barriers introduced in offices, hospitals, etc. so to provide social distancing. Moreover, recycling of PMMA is costful, which can be among the causes for its release into the environment. Finally, PMMA has a well-known and well-studied hydrophobicity-driven interaction with proteins [53], thus it is a convenient model of nanoplastic. The ER-GNG biosensor was tested for its PMMA detection ability initially in aqueous solutions and later in real seawater.

2. Materials and methods

2.1. Chemicals

N-hydroxysuccinimide (NHS) (6066-82-6), N-(3-dimethylaminopropyl)-N'-ethylcarbodiimide hydrochloride (EDC) (25952-53-8), α-lipoic acid (1077-28-7), 2,2'-Azobis(isobutyronitrile) (441090), ethanolamine (141-43-5), phosphate buffer saline 10 mM, pH 7.4 (PBS) (MFCD00131855), 2-(N-morpholino)ethanesulfonic acid (MES) (4432-31-9), sodium chloride (7647-14-5) were purchased from Sigma-Aldrich (Darmstadt, Germany). Recombinant Human Estrogen Receptor alpha protein (ER) (ab82606 abcam) was purchased from Abcam (Cambridge, UK). Spherical poly(methyl methacrylate) (PMMA) nanoplastics (100 nm) (DNP-P034) and spherical microplastic (20 μm) (DMN-L015) were purchased from CD Bioparticles (London, UK) as standard aqueous stock solution (10 mg/ml). All chemicals were used without further purification.

2.2. The GNG sensor chip

The GNG-based plasmonic platform production process is reported in details in Refs. [51,52]. A 10 mm × 10 mm × 0.5 mm PMMA slab waveguide (GoodFellow, Huntingdon, England) was spin-coated with a positive PMMA e-beam resist (AR-P 679.04, AllResist GmbH, Strausberg, Germany) at 6000 rpm for 1 min, to reach a final thickness of about 220 nm. Next, the exposition process was performed by means of an electron beam lithography system (Zeiss Supra v35—Raith Elphy Quantum, Oberkochen, Germany). The area processed was 1 mm^2 (1 mm × 1 mm) and was located at the center of the slab waveguide. The exposed resist was then developed and, as a final step, a 40 nm thick gold film was sputtered (Safematic CCU-010, Zizers, Switzerland) on the top. The selected geometrical parameters for the nanograting were according to previous optimizations [52], i.e. each nanostripe had a 400 nm width and the spacing between contiguous nanostripes was of about 600 nm. Overall, the grating period was equal to about 1 μm.

2.3. ER functionalization protocol

The functionalization of the plasmonic platforms was performed *via* a multi-steps process, according to the protocol reported in Refs. [54,55]. At first, the surface was washed with Milli-Q water (3 times). Then the gold nanofilm was treated overnight at room temperature with α-lipoic acid (0.3 mM in 8% ethanolic solution) Then, the carboxylic groups were activated with EDC/NHS (10 mM/10 mM respectively) in MES buffer 50 mM pH 5.5, for 20 min at room temperature, according to the coupling protocol optimized in Refs. [54,55]. After washing three times to remove the reactant in excess, the surface was incubated for 2 h with ER (13 ng) at room temperature in a sealed humid box. Finally, the passivation of the surface was performed by incubating ethanolamine (1 mM in water) for 30 min at room temperature. The prepared platforms were washed in PBS and stored in PBS at 4 °C.

2.4. Sensor setup

To test plasmonic platforms, a simple experimental setup consisting of a halogen lamp as white light source with an emission range 360–1700 nm (HL-2000LL, Ocean Insight, Orlando, FL, USA) and a spectrometer with a detection range 350–1000 nm (FLAME-S-VIS-NIR-ES, Ocean Insight, Orlando, FL, USA) was used. This allowed to excite the plasmonic hybrid modes in the GNG [51,52]. Fig. 1 provides the details of the plasmonic platform setup. GNG-plasmonic platform was placed into a specially designed aluminium holder: the light was launched from the source to a first plastic optical fiber (POF) patch (1 mm total diameter). At the end of the POF, a trench of air was realized in the metallic holder, in order to increase the number of angles to excite plasmons in the nanograting-based slab waveguide. Another POF patch (1 mm total diameter), orthogonally placed with respect to the air trench, was used to collect the transmitted light through the nanostructured slab waveguide and to send it to the spectrometer. To achieve the best performances, the stripes forming the nanograting pattern were oriented along the same direction of the light input [51]. Moreover, a thermo-stabilized chambers with humidity control were realized to avoid samples evaporation.

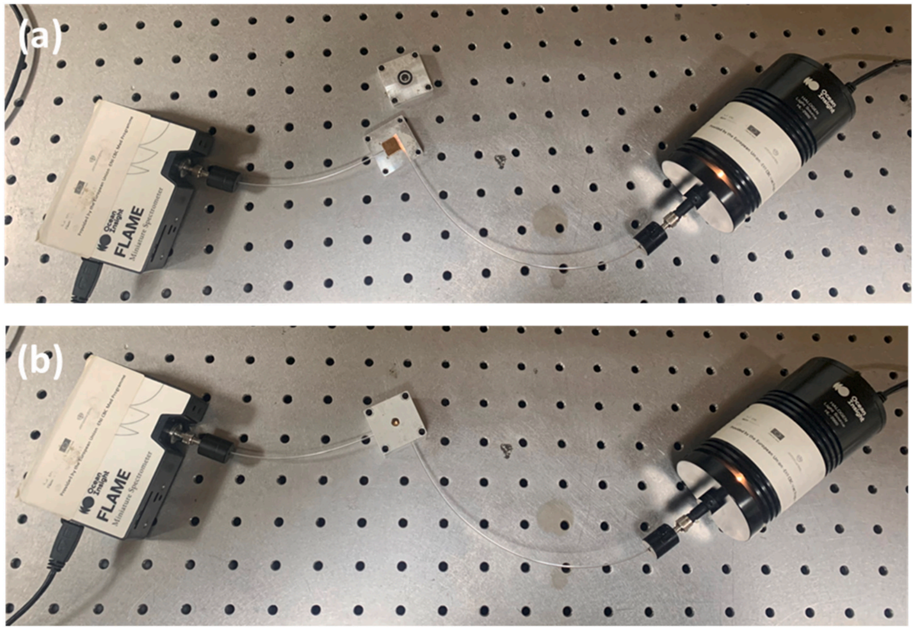

Fig. 1. Experimental setup of the ER-GNG biosensor. The pictures show the measuring chambers when **a)** open and **b)** capped.

2.5. Measurements procedure

Prior to measurements, the nanoplastic (100 nm) stock solution was diluted to the final tested concentrations (1 ng/mL to 1 mg/mL) with PBS or with simulated seawater (0.46 M of NaCl in MilliQ water). Prior the use, all solutions were sonicated for ~15 min to ensure nanoplastics were dispersed homogenously. The seawater samples were collected in glass tubes from Naples's area (Giugliano in Campania). Sampling was carried out just below the surface of the sea. The seawater was diluted with PBS 1:20 before testing.

A sample's volume of 2 μL was used for measurement with an incubation time of 3 min. The incubation times were defined according to preliminary binding kinetics information (see Figure S1 of Supplementary Material). The plasmonic spectra were collected after a washing step with PBS and by placing PBS (2 μL) as bulk solution. The spectrum acquired with air as surrounding medium was considered as a reference for the normalization, being this a condition in which the plasmonic phenomenon is not triggered [51].

Phosphate buffer saline (pH 7.4) was used for the measurements to control and optimize the interaction between the nanoplastic and the ER, as pH values far from the physiological one (pH 7.4) are reported to reduce the binding activity [56].

Moreover, being the sensor based on the ER recognition element, that has been herein exploited to recognize nanoplastics, typically characterized by a variety of sizes and compositions, the experimental data were fitted with the Hill model equation, which describes heterogeneous binding, and has the general formula herein reported. On the contrary, when the receptor was tested for the binding to its own target (Estradiol) the binding isotherm was described by a Hill model with n = 1, which de facto represents the Langmuir model, as reported in Ref. [55]. Hill model has the general formula reported below:

$$|\Delta\lambda| = |\lambda_c - \lambda_0| = |\Delta\lambda_{max}| \cdot \left(\frac{c^n}{{EC_{50}}^n + c^n} \right) \quad (1)$$

where λ_c is the resonance wavelength at the analyte concentration c; λ_0 is the resonance wavelength in absence of the analyte (blank); $\Delta\lambda_{max}$ is the maximum value of $\Delta\lambda$; calculated by subtracting the blank value from the saturation value; n is the Hill coefficient and EC_{50} is the ligand concentration at half saturation. Error bars were calculated as the maximum experimentally measured variation, obtained by testing three similar platforms in a similar condition, and resulted to be equal to about 0.2 nm.

2.6. Standard method for determination of nanoplastics

The concentration of nanoplastics in a real seawater sample was verified with a standard method [57]. Samples were subjected to consecutive filtrations onto 0.8 μm and 0.22 μm cellulose acetate syringe filters (Millex-HA) to remove the macroparticles, sand and organic matter. The filtered samples were next passed on a 0.02 μm syringe filter (Whatman Anotop) in order to retain the nanoplastics. The filter was then thoroughly washed with MilliQ water in order to remove all the residual salts and placed in oven at 45 °C until completely dry. Finally, the filters were weighted on an analytical balance (Shimadzu AUW220D).

3. Results

With the aim to determine the nanoplastic concentration in waters, a plasmonic sensors based on the ER as selective element was herein developed. In an early phase the ER was coupled with a SPR plastic optical fiber platform (SPR-POF) [58] (data not shown). These first results showed the ER-SPR-POF enabled to monitor nanoplastics in PBS and in simulated seawater in the range of concentration 1–10 mg/mL, possibly as a consequence of the RI of the nanoplastic suspensions at these concentrations, whose supposed effect was to modify the RI at the sensing surface, in line with [48]. Such a sensor's response did not appear to satisfy the request of real scenarios, as previous case studies on melt snow and seawaters reported an estimated nanoplastic concentration in the order of the tens of ng/mL [11,59,60]. In order to meet lower sensitivities (ng/mL) and avoid sample preconcentration steps, a high performing plasmonic transducing element was functionalized with the same receptor. Indeed, the surface of the highly sensitive GNG transducer [51] was modified with the ER receptor, reported to interact with high affinity to microplastics [49], with the aim to devise a biosensor suitable for the ng/mL detection of nanoplastics. The GNG platforms was produced as reported in detail in Refs. [51,52], and the production steps are depicted in the scheme of Fig. 2a. Fig. 2b and c shows respectively the scanning electron microscopy (SEM) image of the fabricated GNG and the actual image of the GNG-based plasmonic chip. Then, the

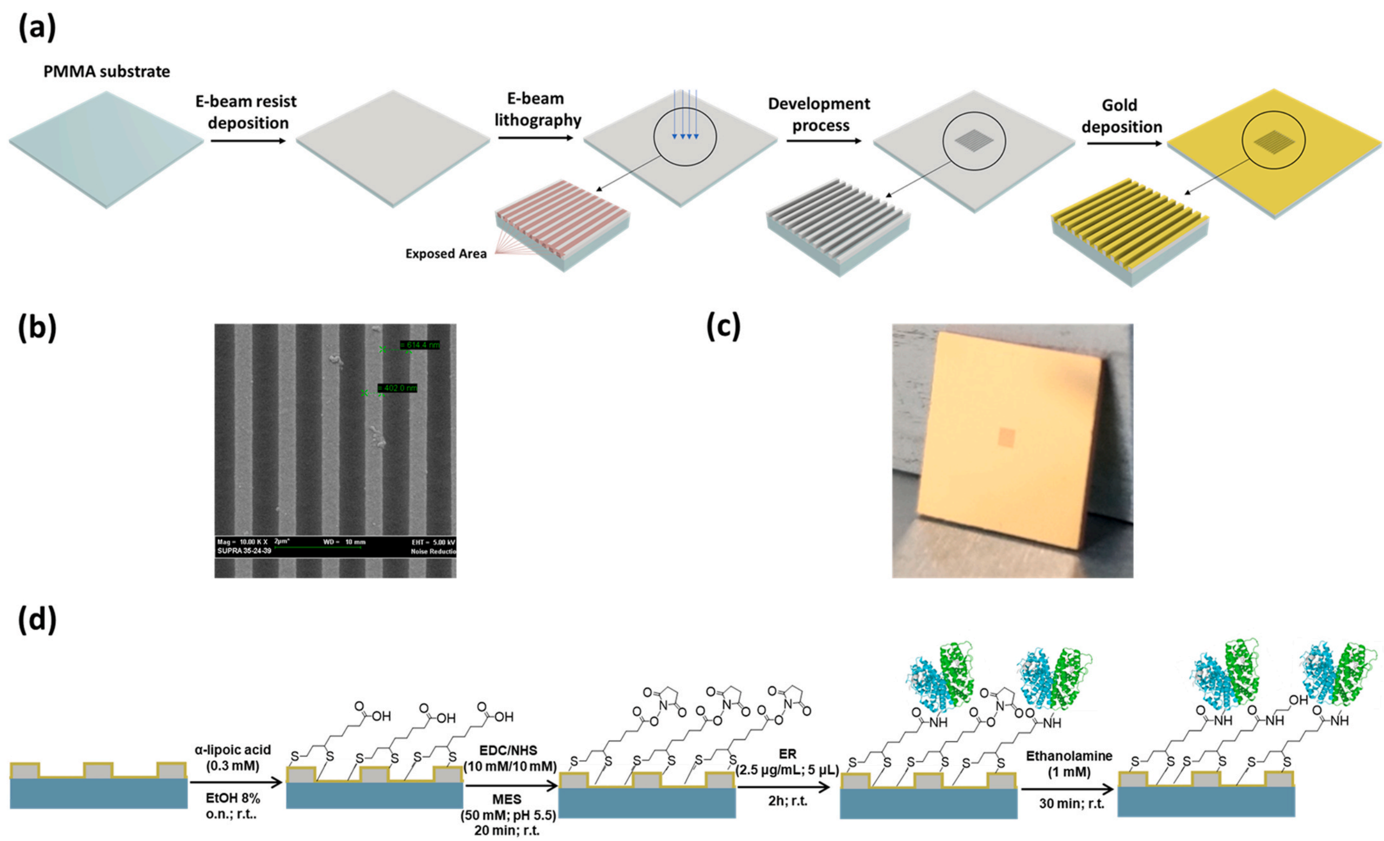

Fig. 2. **a)** Scheme of GNG-based chip production processes **b)** SEM image of the GNG. **c)** Photo of GNG-based platform [51]. **d)** Scheme of coupling reactions.

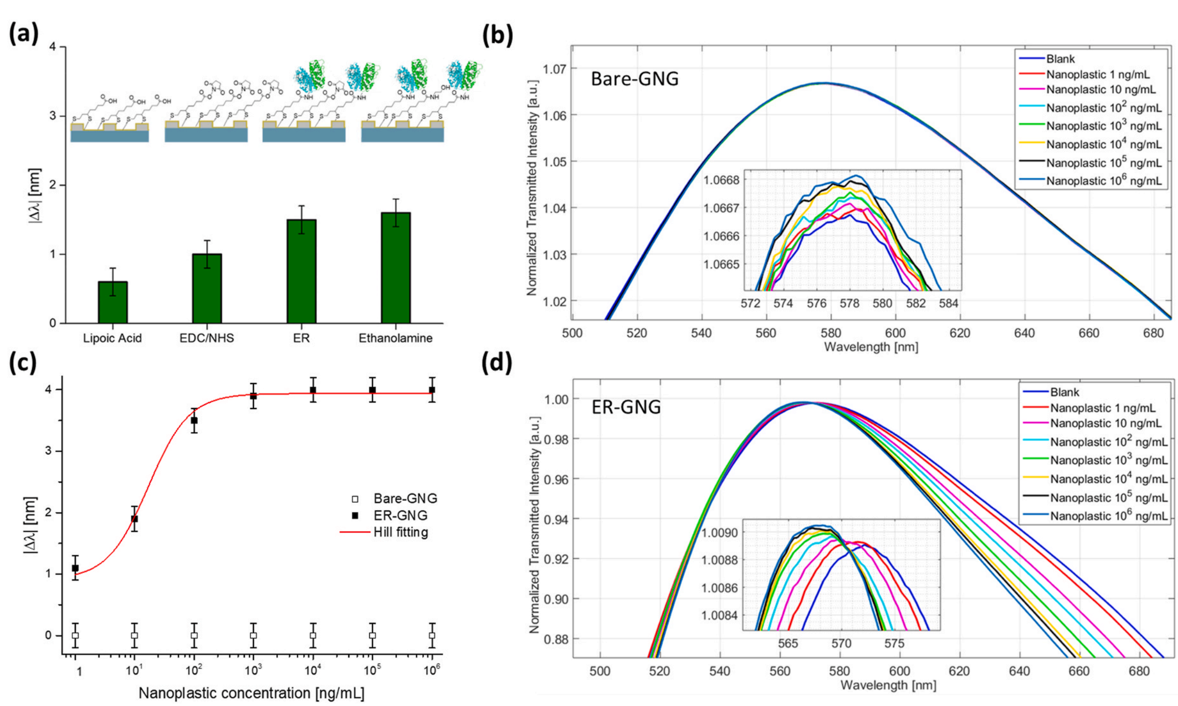

Fig. 3. ER-GNG platform. **a)** Absolute value of the variation in resonance wavelength (blue shift), calculated with respect to the bare chip considering PBS as surrounding medium, after each step of the functionalization process on ER-GNG (n = 3, SD = 0.2 nm). **b)** Normalized plasmonic spectra relative to nanoplastics detection in PBS at different concentrations on bare nanostructured platform. **c)** Absolute value of the variation in resonance wavelength as a function of the nanoplastics concentration in semi-log scale on bare (□) and functionalized (■) platform and fitting of the experimental data. (n = 3, SD = 0.2 nm). **d)** Normalized plasmonic spectra relative to nanoplastics detection in PBS at different concentrations on ER-GNG platform.

platform surface was functionalized with ER by a multi-step protocol, described in details in Refs. [54,55]. The functionalization steps are schematically reported in Fig. 2d. The gold surface was treated with α-lipoic acid to let the thiol groups react with the gold and form a self-assembled monolayer (SAM) with exposed the terminal carboxylic groups. Next the carboxylic moieties were activated with EDC/NHS and ER was covalently coupled to the SAM through the formation of an amide bond between the α-lipoic acid carboxylic group and ER amine group [55], obtaining a randomly oriented ER functionalized surface. Finally, the surface was passivated, in order to quench unreacted activated carboxylic groups.

The successful completion of each functionalization step was monitored by the changes in the plasmonic spectra calculated with respect to the bare platform (without receptor) considering PBS as a surrounding medium. As shown in Fig. 3a changes in term of resonance wavelength, in presence of the same surrounding medium's RI (i.e., PBS) were observed after each functionalization step (spectra reported in Figure S2 of Supplementary Material), confirming surface modifications. The functionalization steps on the GNG platform produced a decrease in resonance wavelength (blue shift). This optical shifts towards shorter wavelengths can be ascribed to the optical phenomena taking place in the used platforms, since GNG relies on the excitation and mutual interaction of SPR and LSPR phenomena [51,52]. These assumptions are supported by the fact that surrounding media with higher RI placed on the plasmonic surface gave rise to the resonance wavelength values that decreased (blue-shift) [51].

The ER-GNG biosensor's response for the nanoplastics was tested in PBS in the range of concentrations between 1 ng/mL and 1 mg/mL at the incubation time of 3 min (see Figure S1 of Supplementary Material). As shown in Fig. 3d, the plasmonic spectra, normalized to the reference spectrum, exhibit a decrease of the plasmonic resonance wavelength by increasing the nanoplastic concentration. Fig. 3c reports the binding isotherm for the nanoplastics on ER-GNG, i.e. the absolute value of the resonance wavelength variation ($|\Delta\lambda|$) calculated with respect to the blank (PBS solution without analyte) *versus* the nanoplastics concentration in semi-log scale. The experimental data were fit by means of the Hill model equation (Equation (1)). Table 1 reports the fitting parameters.

As a control, the response of a bare platform was tested (Fig. 3b and c) showing no resonance wavelength variation, thus confirming the specificity of the sensor response.

Additionally, the ER-GNG biosensor's response was tested for the same nanoplastics concentration range (1 ng/mL–1 mg/mL) in simulated seawater. Fig. 4a reports the normalized plasmonic spectra for increasing nanoplastics concentration. Binding confirmed the blue-shift, in agreement to measurements in PBS and to Ref. [51], as shown in Fig. 4a, whereas Fig. 4b reports the Hill fitting of the experimental data. The Hill model fitting parameters obtained in both PBS and simulated seawater are reported in Table 1. The comparison between the parameters for the measurements on the ER-GNG sensor in PBS and in simulated seawater demonstrated that the platform's response was slightly influenced by the matrix variation. Hence, the sensor permits to determine nanoplastics both in PBS and seawater. Moreover, the ER-GNG biosensor response was in the range of concentrations of interest for the screening of real samples.

Table 1
Hill parameters of nanoplastic detection on ER-GNG sensor in PBS and in seawater.

ER-GNG	$\Delta\lambda_0$ [nm]	$\Delta\lambda_{max}$ [nm]	EC_{50} [ng/mL]	n	Statistics: Reduced χ^2	Statistics: Adj. R^2
PBS	−0.98 ± 0.03	3.99 ± 0.01	21.80 ± 1.02	1.02 ± 0.04	0.02	0.999
seawater	0.44 ± 0.02	3.51 ± 0.15	52.50 ± 49.80	0.43 ± 0.13	0.48	0.981

The analytical parameters of ER-GNG sensor are reported in Table 2. The remarkable performance, in term of LOD, can be mainly ascribed to the kind of excited plasmonic phenomenon in the GNG-based platform. In fact, the mutual interactions between SPR and LSPR phenomena, triggered on the GNG surface, give rise to hybrid plasmonic modes [51,52,61,62]. In such a way, since the nanoplastic to ER binding event takes place in close proximity to the gold nanostructures, a noticeable improvement in terms of binding sensitivity is achieved [51].

At last, as a proof of concept the ER-GNG biosensor was tested with a real seawater sample collected from Naples area. The sample was diluted 1:20 in PBS and it was tested without any kind of sample pretreatment. The dilution ratio was chosen arbitrarily in order to limit the influence on the measurement of non-physiologic pHs. The 1:20 dilution ensured to reduce the seawater pH from >8.0 to 7.4, while allowing a good trade-off between the pH effect correction and maintaining the concentration of the nanoplastics above the LOD, thus avoiding preconcentration process.

The plasmonic spectrum relative to the real sample reported in Fig. 5 (magenta spectrum), shows a clear blue-shift of the resonance wavelength with respect to the blank (blue spectrum). From the calibration curve in Fig. 4b and from the resonance wavelength shift observed, it was possible to estimate the concentration of nanoplastics in the real seawater sample (Fig. 5b). The obtained value (1.5 ng/mL) was multiplied by the dilution factor yielding to estimate the concentration of nanoplastic in the seawater sample equal to 30 ng/mL.

To confirm the ER-GNG sensor's determined value, the residual weight of the seawater sample was measured after consecutive filtrations and evaporation treatments [57]. The estimated nanoplastics concentration, as per the obtained weight, was ~53 ng/mL and it showed a good degree of agreement with the ER-GNG results obtained, demonstrating the validity of the herein proposed sensing approach.

A further experiment was intended at evaluating whether the ER-GNG sensor was able to discriminate between nano- and microplastics. To this purpose the binding kinetics for micro- and nanoplastics, both considered at the same concentration (1 ng/mL), were evaluated monitoring the spectral shift at different times in presence of micro- and nanoplastics. As shown in Fig. 6 the spectral shifts at 3 min for both nano- and microplastic showed that nanoplastics produced a significantly more pronounced shift ($|\Delta\lambda| = 1.10$ nm) respect to microplastics ($|\Delta\lambda| = 0.18$ nm), hence indicating that the incubation time can be exploited to select nanoplastic over microplastics.

Finally, reusability, reproducibility, and repeatability of sensor was evaluated. After each measurement, the ER-GNG biosensor was regenerated by extensive washings with PBS while the storage was at 4 °C in PBS. The regeneration process of the proposed ER-functionalized surface was effective, as shown by the constant sensor's response (100%) after regeneration cycles ($n = 4$). In a wider study, the ER-GNG was tested for its reusability, by monitoring the response over a period of three months. Fig. 7 shows the efficiency of the regeneration cycles over time for the same platform. In particular, Fig. 7a reports the variation in resonance wavelength ($\Delta\lambda$) normalized to the maximal response, i.e. obtained at the first use ($\Delta\lambda_{max}(t_0)$), for several binding (grey background) and regeneration (blue background) cycles on the same functionalized platform at the different weeks of utilization. The sensor response recovery was calculated as percentage of variation in resonance wavelength normalized to the maximal response, i.e. obtained at the first use, for binding at a fixed concentration (1 ng/mL). Fig. 7b shows that the sensor response was fully recovered in the first two weeks of utilization, after 4 regeneration's cycles (plasmonic spectra are reported in Figure S3 of Supplementary Material). Then a progressive worsening of the response was observed.

Repeatability tests were performed, within the first two weeks of utilization, on the same platform in the same conditions ($n = 10$), and the maximum experimentally measured variation in plasmonic resonance wavelength was equal to 0.2 nm. The reproducibility of the ER-

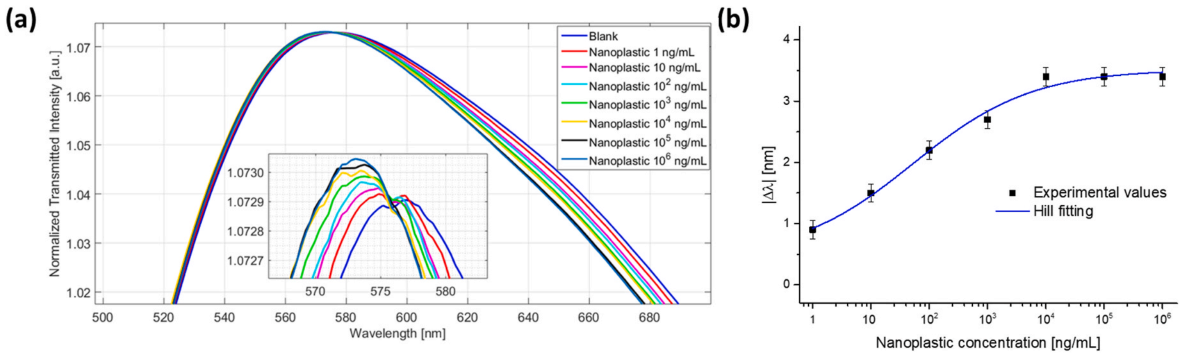

Fig. 4. **a)** Normalized plasmonic spectra relative to nanoplastics detection in simulated seawater at different concentrations on ER-GNG biosensor. **b)** Absolute value of the variation in resonance wavelength as a function of the nanoplastics concentration in semi-log scale and fitting of the experimental data (n = 3, SD = 0.2 nm).

Table 2
ER-GNG analytical parameters relative to nanoplastics detection.

ER-GNG	Sensitivity at low concentration ($\lvert\Delta\lambda_{max} - \Delta\lambda_0\rvert/EC_{50}$)	LOD[a] (3[a]standard deviation of blank/sensitivity at low concentration)
In PBS	0.230 nm/ng mL^{-1}	0.39 ng/mL
In seawater	0.059 nm/ng mL^{-1}	1.02 ng/mL

[a] **From** [63].

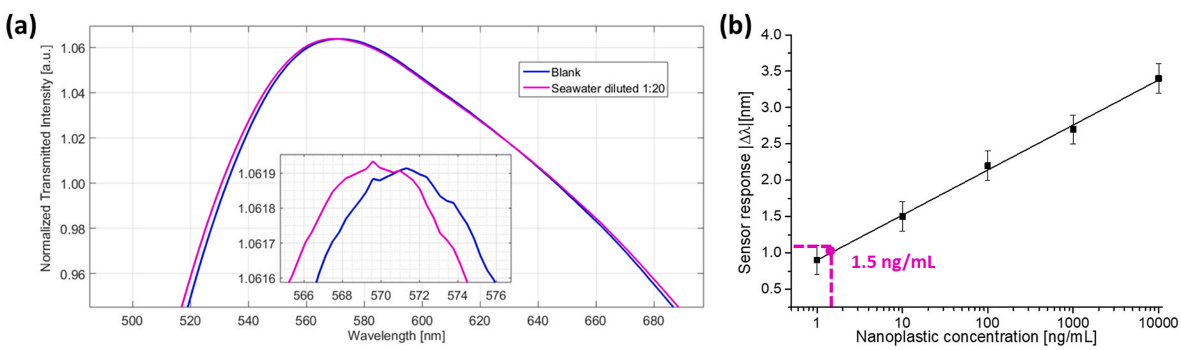

Fig. 5. **a)** Normalized plasmonic spectra relative to nanoplastics detection in real seawater sample solution on ER-GNG **b)** Extrapolation of concentration in real seawater diluted 1:20 from the calibration curve.

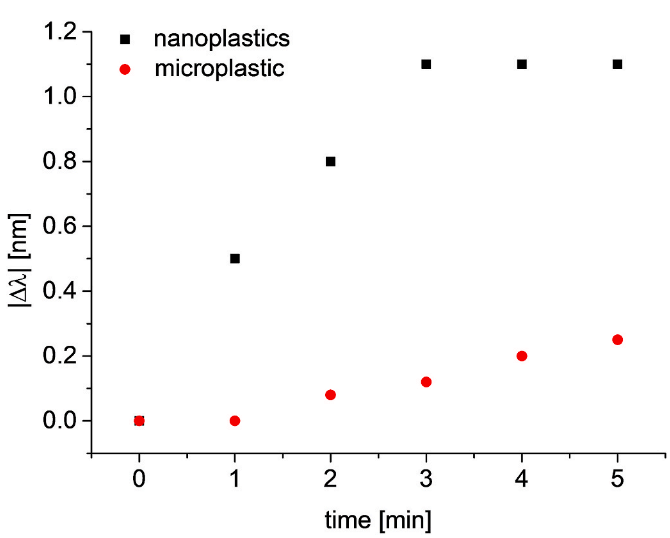

Fig. 6. Absolute value of variation in resonance wavelength ($|\Delta\lambda|$) as a function of incubation time for micro- (●) and nanoplastic (■) both considered at the same concentration (1 ng/mL).

GNG biosensor was tested on three different platforms in similar conditions (n = 3), and the maximum discrepancy in resonance wavelength resulted equal to 0.2 nm.

Moreover, a comparison between the nanoplastics sensing strategies reported in the literature and the ER-GNG, reported in Table 3, showed that the ER-GNG sensor displays equal when not superior performance. In fact, few sensing techniques showed similar LODs whereas most displayed to respond for concentrations of nanoplastics far from the expected levels in the environment.

4. Discussion and conclusions

In this work, we reported the development of a proof of concept nanoplastic sensor, exploiting a gold nanostructured plasmonic biosensor, devised by coupling the ER receptor to a GNG chip. The GNG structure was based on a previously optimized polymer-based sensor's configuration [51,52]. Various metals, e.g. silver, may be used to excite the plasmonic phenomena, but the gold-ones were herein preferred, because gold deposition is state-of-art and, additionally, it does not oxidize over time, thus extending the device durability and reusability.

Concerning the recognition element, the ER receptor was chosen from studies reported in the literature, which indicated the ER as a suitable element for the detection of microplastics [49] but in a concentration range far from the expected real scenario. The distinctive

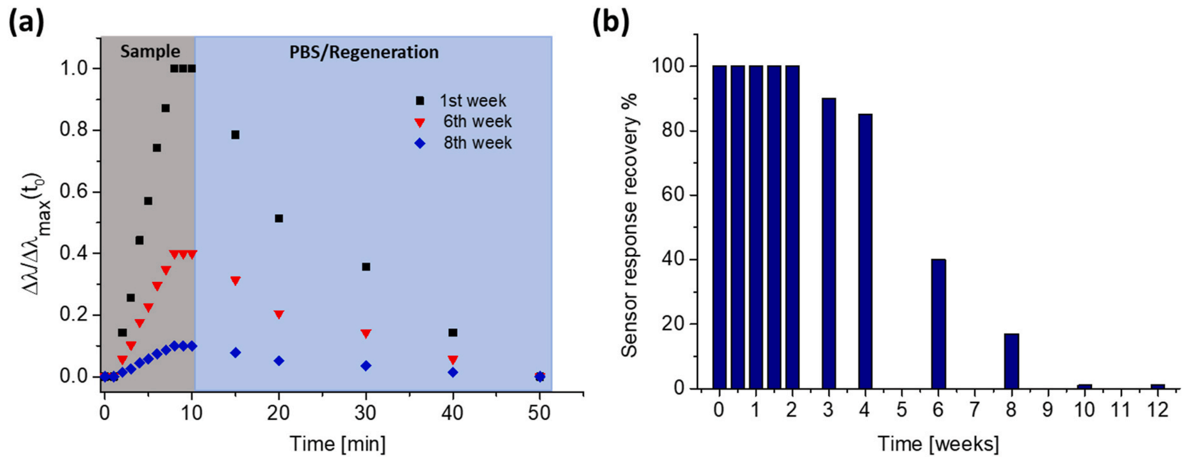

Fig. 7. **a)** Resonance wavelength variation (Δλ) normalized to the maximal response obtained at the first use ($\Delta\lambda_{max}(t_0)$) as a function of time, during the binding (grey background) and the regeneration step (blue background). **b)** Sensor response recovery (%) over time.

Table 3
Comparison between several sensing techniques for nanoplastics detection.

Sensing Technique	LOD	REF
Surface Enhanced Raman Scattering (SERS)	10 μg/mL	[64]
Optical Tweezers coupled with Raman	<1 μg/mL	[65]
LSPR sandwich	1 μg/mL	[66]
Differential Pulse Voltammetry (DPV) sandwich	0.90 ng/mL	[67]
ER-GNG	0.39 ng/mL	This work

feature of the ER-GNG sensor, was the choice of the nanoplasmonic transducer, which conferred superior binding sensitivity [51,52] and thus avoided the need for sample pre-treatment. Indeed, the proposed ER-GNG biosensor required just 2 μL of sample, produced a response within 3 min and showed sensitivity for the detection of nanoplastics in real environmental ranges of concentrations. The ER-GNG sensor appeared to allow the determination of nanoplastics in seawater samples without any sample pre-treatment. Moreover, the nanoplastics concentration measured with ER-GNG (equal to about 30 ng/mL) was then confirmed by a conventional method, consisting of the recovery of nanoplastics in the seawater samples through filtration, demonstrating a good overlapping of the results. Overall, the ER-GNG sensor appeared to match the requirements imposed by a real scenario, considering that its lifetime is around two weeks.

As there are no standardized procedures and regulations for nanoplastics, while recent scientific literature [68] proposes criteria, applying the ER-GNG sensor to other matrices of interest (e.g., tap water, blood sample, food, etc.) in environmental and biomedical fields would contribute to clarifying the extent of the issue of the contamination derived by nanoplastics and possibly contribute to setting the regulations.

CRediT authorship contribution statement

Mimimorena Seggio: Investigation, Methodology, Data curation, Writing – original draft. **Francesco Arcadio**: Investigation, Data curation, Writing – original draft. **Cennamo Nunzio**: Conceptualization, Methodology, Supervision, Writing – original draft, Writing – review & editing. **Luigi Zeni**: Supervision, Funding acquisition, Writing – review & editing. **Alessandra Maria Bossi:** Conceptualization, Methodology, Funding acquisition, Supervision, Writing – original draft, Writing – review & editing.

Declaration of competing interest

The authors declare that they have no known competing financial interests or personal relationships that could have appeared to influence the work reported in this paper.

Data availability

Data will be made available on request.

Acknowledgements

MS and AMB thanks the Italian Ministry of University for the Project DM 1062 2021 "Ricercatori a Tempo Determinato di tipo A (RTDA) Azione IV.6 - Contratti di ricerca su tematiche Green" [40-G-15185-5]; MS thanks Optosensing s. r.l. for hosting her as visiting researcher. This work has been done in part within the research program “Dipartimento di Eccellenza 2023–2027” awarded to Dipartimento di Biotecnologie of the Università di Verona.

Appendix A. Supplementary data

Supplementary data to this article can be found online at https://doi.org/10.1016/j.talanta.2023.125211.

References

[1] R. Geyer, J.R. Jambeck, K.L. Law, Production, use, and fate of all plastics ever made, Sci. Adv. 3 (2017), 1700782, https://doi.org/10.1126/sciadv.1700782.
[2] PlasticsEurope, Plastics—The Facts 2019. An Analysis of European Plastics Production, Demand and Waste Data, PlasticsEurope, Brussels, Belgium, 2019.
[3] A. Bianco, F. Sordello, M. Ehn, D. Vione, M. Passananti, Degradation of nanoplastics in the environment: reactivity and impact on atmospheric and Surface Waters, Sci. Total Environ. 742 (2020), 140413, https://doi.org/10.1016/j.scitotenv.2020.140413.
[4] T. Bond, V. Ferrandiz-Mas, M. Felipe-Sotelo, E. van Sebille, The occurrence and degradation of aquatic plastic litter based on polymer physicochemical properties: a Review, Crit. Rev. Environ. Sci. Technol. 48 (2018) 685–722, https://doi.org/10.1080/10643389.2018.1483155.
[5] A.L. Dawson, S. Kawaguchi, C.K. King, K.A. Townsend, R. King, W.M. Huston, S. M. Bengtson Nash, Turning microplastics into nanoplastics through digestive fragmentation by Antarctic krill, Nat. Commun. 9 (2018) 1001, https://doi.org/10.1038/s41467-018-03465-9.
[6] I.E. Napper, R.C. Thompson, Environmental deterioration of biodegradable, oxo-biodegradable, compostable, and conventional plastic carrier bags in the sea, soil, and open-air over a 3-year period, Environ. Sci. Technol. 53 (2019) 4775–4783, https://doi.org/10.1021/acs.est.8b06984.
[7] J.S. Vicente, J.L. Gejo, S. Rothenbacher, S. Sarojiniamma, E. Gogritchiani, M. Wörner, G. Kasperb, A.M. Braun, Oxidation of polystyrene aerosols by VUV-photolysis and/or ozone, Photochem. Photobiol. Sci. 8 (2009) 944–952, https://doi.org/10.1039/b902749a.

[8] M. Wagner, C. Scherer, D. Alvarez-Muñoz, N. Brennholt, X. Bourrain, S. Buchinger, E. Fries, C. Grosbois, J. Klasmeier, T. Marti, S. Rodriguez-Mozaz, R. Urbatzka, D. Vethaak, M. Winther-Nielsen, G. Reifferscheid, Microplastics in freshwater ecosystems: what we know and what we need to know, Environ. Sci. Eur. 26 (2014) 12, https://doi.org/10.1186/s12302-014-0012-7.

[9] A.A. Koelmans, N.H. Mohamed Nor, E. Hermsen, M. Kooi, S.M. Mintenig, J. De France, Microplastics in freshwaters and drinking water: critical Review and assessment of Data, Quality Water Res 155 (2019) 410–422, https://doi.org/10.1016/j.watres.2019.02.054.

[10] M. Bergmann, S. Mützel, S. Primpke, M.B. Tekman, J. Trachsel, G. Gerdts, White and wonderful? Microplastics prevail in snow from the Alps to the Arctic, Sci. Adv. 5 (2019) 1157, https://doi.org/10.1126/sciadv.aax1157.

[11] D. Materić, A. Kasper-Giebl, D. Kau, M. Anten, M. Greilinger, E. Ludewig, E. van Sebille, T. Röckmann, R. Holzinger, Micro- and nanoplastics in Alpine snow –a new method for chemical identification and quantification in the nanogram range, Environ. Sci. Technol. 54 (2020) 2353–2359, https://doi.org/10.1021/acs.est.9b07540.

[12] M. Parolini, D. Antonioli, F. Borgogno, M.C. Gibellino, J. Fresta, C. Albonico, J. Fresta, C. Albonico, B. De Felice, S. Canuto, D. Concedi, A. Romani, E. Rosio, V. Gianotti, M. Laus, R. Ambrosini, R. Cavallo, Microplastic contamination in snow from western Italian Alps, Int. J. Environ. Res. Publ. Health 18 (2021) 768, https://doi.org/10.3390/ijerph18020768.

[13] L.D.K. Kanhai, K. Gardfeldt, T. Krumpen, R.C. Thompson, I. O'Connor, Microplastics in sea ice and seawater beneath ice floes from the Arctic Ocean, Sci. Rep. 10 (2020) 5004, https://doi.org/10.1038/s41598-020-61948-6.

[14] R. Ambrosini, R.S. Azzoni, F. Pittino, G. Diolaiuti, A. Franzetti, M. Parolini, First evidence of microplastic contamination in the supraglacial debris of an Alpine Glacier, Environ. Pollut. 253 (2019) 297–301, https://doi.org/10.1016/j.envpol.2019.07.005.

[15] A. Kelly, D. Lannuzel, T. Rodemann, K.M. Meiners, H.J. Auman, Microplastic contamination in east antarctic sea ice, Mar. Pollut. Bull. 154 (2020), 111130, https://doi.org/10.1016/j.marpolbul.2020.111130.

[16] D. Allen, S. Allen, G. Le Roux, A. Simonneau, D. Galop, V.R. Phoenix, Temporal Archive of atmospheric microplastic deposition presented in ombrotrophic peat, Environ. Sci. Technol. Lett. 8 (2021) 954–960, https://doi.org/10.1021/acs.estlett.1c00697.

[17] M.C. Rillig, R. Ingraffia, A.A. de Souza Machado, Microplastic incorporation into soil in Agroecosystems, Front. Plant Sci. 8 (2017) 8–11, https://doi.org/10.3389/fpls.2017.01805.

[18] C. Wahl, Le Juge, M. Davranche, H. El Hadri, B. Grassl, S. Reynaud, J. Gigault, Nanoplastic occurrence in a soil amended with plastic debris, Chemosphere 262 (2021), 127784, https://doi.org/10.1016/j.chemosphere.2020.127784.

[19] M. Bergmann, V. Wirzberger, T. Krumpen, C. Lorenz, S. Primpke, M.B. Tekman, G. Gerdts, High quantities of microplastic in arctic deep-sea sediments from the Hausgarten Observatory, Environ. Sci. Technol. 51 (2017) 11000–11010, https://doi.org/10.1021/acs.est.7b03331.

[20] M. Chen, M. Du, A. Jin, S. Chen, S. Dasgupta, J. Li, H. Xu, K. Ta, X. Peng, Forty-year pollution history of microplastics in the largest marginal sea of the Western Pacific, Geochem. Perspect. Lett. (2020) 42–47, https://doi.org/10.7185/geochemlet.2012.

[21] J. Martin, A.L. Lusher, F.C. Nixon, A review of the use of microplastics in reconstructing dated Sedimentary Archives, Sci. Total Environ. 806 (2022), 150818, https://doi.org/10.1016/j.scitotenv.2021.150818.

[22] F. Büks, N. Loes van Schaik, M. Kaupenjohann, What do we know about how the terrestrial multicellular soil fauna reacts to microplastic? Soils 6 (2020) 245–267, https://doi.org/10.5194/soil-6-245-2020.

[23] E. Huerta Lwanga, H. Gertsen, H. Gooren, P. Peters, T. Salánki, M. van der Ploeg, E. Besseling, A.A. Koelmans, V. Geissen, Incorporation of microplastics from litter into burrows of Lumbricus terrestris, Environ. Pollut. 220 (2017) 523–531, https://doi.org/10.1016/j.envpol.2016.09.096.

[24] S. Krause, V. Baranov, H.A. Nel, J.D. Drummond, A. Kukkola, T. Hoellein, G. H. Sambrook Smith, J. Lewandowski, B. Bonet, A.I. Packman, J. Sadler, V. Inshyna, S. Allen, D. Allen, L. Simon, F. Mermillod-Blondin, I. Lynch, Gathering at the top? environmental controls of microplastic uptake and biomagnification in freshwater food webs, Environ. Pollut. 268 (2021), 115750, https://doi.org/10.1016/j.envpol.2020.115750.

[25] M.C. Rillig, A. Lehmann, A.A. Souza Machado, G. Yang, Microplastic effects on plants, New Phytol. 223 (2019) 1066–1070, https://doi.org/10.1111/nph.15794.

[26] S. Allen, D. Allen, V.R. Phoenix, G. Le Roux, P. Durántez Jiménez, A. Simonneau, S. Binet, D. Galop, Atmospheric transport and deposition of microplastics in a remote mountain catchment, Nat. Geosci. 12 (2019) 339–344, https://doi.org/10.1038/s41561-019-0335-5.

[27] J. Brahney, N. Mahowald, M. Prank, G. Cornwell, Z. Klimont, H. Matsui, K. H Prather, Constraining the atmospheric limb of the plastic cycle, Proc. Natl. Acad. Sci. USA 118 (2021), https://doi.org/10.1073/pnas.2020719118.

[28] R. Dris, J. Gasperi, C. Mirande, C. Mandin, M. Guerrouache, V. Langlois, V. Langlois, B. Tassin, A first overview of textile fibers, including microplastics, in indoor and outdoor environments, Environ. Pollut. 221 (2017) 453–458, https://doi.org/10.1016/j.envpol.2016.12.013.

[29] M. Klein, E.K. Fischer, Microplastic abundance in atmospheric deposition within the metropolitan area of Hamburg, Germany, Sci. Total Environ. 685 (2019) 96–103, https://doi.org/10.1016/j.scitotenv.2019.05.405.

[30] S.L. Wright, J. Ulke, A. Font, K.L.A. Chan, F.J. Kelly, Atmospheric microplastic deposition in an urban environment and an evaluation of transport, Environ. Int. 136 (2020), 105411, https://doi.org/10.1016/j.envint.2019.105411.

[31] K. Mattsson, L.-A. Hansson, T. Cedervall, Nano-plastics in the aquatic environment, Environ. Sci.: Process. Impacts 17 (2015) 1712–1721, https://doi.org/10.1039/c5em00227c.

[32] B. Worm, H.K. Lotze, I. Jubinville, C. Wilcox, J. Jambeck, Plastic as a persistent marine pollutant, Annu. Rev. Environ. Resour. 42 (2017) 1–26, https://doi.org/10.1146/annurev-environ-102016-060700.

[33] C. Tagesson, R. Sjödahl, B. Thorén, Passage of molecules through the wall of the gastrointestinal tract, Scand. J. Gastroenterol. 13 (1978) 519–524, https://doi.org/10.3109/00365527809181758.

[34] M. Qu, Y. Qiu, Y. Kong, D. Wang, Amino modification enhances reproductive toxicity of nanopolystyrene on gonad development and reproductive capacity in nematode caenorhabditis elegans, Environ. Pollut. 254 (2019), 112978, https://doi.org/10.1016/j.envpol.2019.112978.

[35] M. Qu, Y. Kong, Y. Yuan, D. Wang, Neuronal damage induced by nanopolystyrene particles in nematode caenorhabditis elegans, Environ. Sci.: Nano 6 (2019) 2591–2601, https://doi.org/10.1039/c9en00473d.

[36] K. Tallec, A. Huvet, C. Di Poi, C. González-Fernández, C. Lambert, B. Petton, et al., Nanoplastics impaired oyster free living stages, gametes and embryos, Environ. Pollut. 242 (2018) 1226–1235, https://doi.org/10.1016/j.envpol.2018.08.020.

[37] O.S. Alimi, J. Farner Budarz, L.M. Hernandez, N. Tufenkji, Microplastics and nanoplastics in aquatic environments: aggregation, deposition, and enhanced Contaminant Transport, Environ. Sci. Technol. 52 (2018) 1704–1724, https://doi.org/10.1021/acs.est.7b05559.

[38] C. Schwaferts, R. Niessner, M. Elsner, N.P. Ivleva, Methods for the analysis of submicrometer- and nanoplastic particles in the environment, TrAC, Trends Anal. Chem. 112 (2019) 52–65, https://doi.org/10.1016/j.trac.2018.12.014.

[39] M. Correia, K. Loeschner, Detection of nanoplastics in food by Asymmetric Flow Field-flow fractionation coupled to multi-angle light scattering: possibilities, challenges and analytical limitations, Anal. Bioanal. Chem. 410 (2018) 5603–5615, https://doi.org/10.1007/s00216-018-0919-8.

[40] C. Capolungo, D. Genovese, M. Montalti, E. Rampazzo, N. Zaccheroni, L. Prodi, Photoluminescence-Based techniques for the detection of micro-and nanoplastics, Chem. Eur J. 27 (2021), 17529.

[41] A.I. Catarino, A. Frutos, T.B. Henry, Use of fluorescent-labelled nanoplastics (NPS) to demonstrate NP absorption is inconclusive without adequate controls, Sci. Total Environ. 670 (2019) 915–920, https://doi.org/10.1016/j.scitotenv.2019.03.194.

[42] R. Gillibert, G. Balakrishnan, Q. Deshoules, M. Tardivel, A. Magazzù, M.G. Donato, O.M. Maragò, M.L. de La Chapelle, F. Colas, F. Lagarde, P.G. Gucciardi, Raman tweezers for small microplastics and nanoplastics identification in seawater, Environ. Sci. Technol. 53 (2019) 9003–9013, https://doi.org/10.1021/acs.est.9b03105.

[43] V. Castelvetro, A. Corti, A. Ceccarini, A. Petri, V. Vinciguerra, Nylon 6 and Nylon 6,6 micro- and nanoplastics: a first example of their accurate quantification, along with polyester (PET), in wastewater treatment plant sludges, J. Hazard Mater. 407 (2021), 124364, https://doi.org/10.1016/j.jhazmat.2020.124364.

[44] V. Castelvetro, A. Corti, S. Bianchi, A. Ceccarini, A. Manariti, V. Vinciguerra, Quantification of poly(ethylene terephthalate) micro- and nanoparticle contaminants in marine sediments and other environmental matrices, J. Hazard Mater. 385 (2020), 121517, https://doi.org/10.1016/j.jhazmat.2019.121517.

[45] L. Wang, J. Zhang, S. Hou, H. Sun, A simple method for quantifying polycarbonate and polyethylene terephthalate microplastics in environmental samples by liquid chromatography–tandem mass spectrometry, Environ. Sci. Technol. Lett. 4 (2017) 530–534, https://doi.org/10.1021/acs.estlett.7b00454.

[46] J. Homola, Present and future of surface plasmon resonance biosensors, Anal. Bioanal. Chem. 377 (2003) 528–539, https://doi.org/10.1007/s00216-003-2101-0.

[47] B. Kaur, S. Kumar, B.K. Kaushik, Recent advancements in optical biosensors for cancer detection, Biosens. Bioelectron. 197 (2022), 113805, https://doi.org/10.1016/j.bios.2021.113805.

[48] J. Tuoriniemi, B. Moreira, G. Safina, Determining number concentrations and diameters of polystyrene particles by measuring the effective refractive index of colloids using surface plasmon resonance, Langmuir 32 (2016) 10632–10640, https://doi.org/10.1021/acs.langmuir.6b02684.

[49] C.-J. Huang, G.V. Narasimha, Y.-C. Chen, J.-K. Chen, G.-C. Dong, Measurement of low concentration of micro-plastics by detection of bioaffinity-induced particle retention using surface plasmon resonance biosensors, Biosensors 11 (2021) 219, https://doi.org/10.3390/bios11070219.

[50] N. Fuentes, P. Silveyra, Estrogen receptor signaling mechanisms, Adv Protein Chem Struct Biol 116 (2019) 135–170, https://doi.org/10.1016/bs.apcsb.2019.01.001.

[51] F. Arcadio, L. Zeni, A. Minardo, C. Eramo, S. Di Ronza, C. Perri, G. D'Agostino, G. Chiaretti, G. Porto, N. Cennamo, A nanoplasmonic-based biosensing approach for wide-range and highly sensitive detection of chemicals, Nanomaterials 11 (2021) 1961, https://doi.org/10.3390/nano11081961.

[52] F. Arcadio, L. Zeni, D. Montemurro, C. Eramo, S. Di Ronza, C. Perri, G. D'Agostino, G. Chiaretti, G. Porto, N. Cennamo, Biochemical sensing exploiting plasmonic sensors based on gold nanogratings and polymer optical fibers, Photon. Res. 9 (2021) 1397, https://doi.org/10.1364/prj.424006.

[53] S. Sathish, N. Ishizu, A.Q. Shen, Air plasma-enhanced covalent functionalization of poly(methyl methacrylate): high-throughput protein immobilization for miniaturized bioassays, ACS Appl. Mater. Interfaces 11 (2019) 46350–46360, https://doi.org/10.1021/acsami.9b14631.

[54] L. Pasquardini, N. Cennamo, G. Malleo, L. Vanzetti, L. Zeni, D. Bonamini, R. Salvia, C. Bassi, A.M. Bossi, A surface plasmon resonance plastic optical fiber biosensor for the detection of pancreatic amylase in surgically-placed drain effluent, Sensors 21 (2021) 3443, https://doi.org/10.3390/s21103443.

[55] F. Arcadio, M. Seggio, L. Zeni, A.M. Bossi, N. Cennamo, Estradiol detection for aquaculture exploiting plasmonic spoon-shaped biosensors, Biosensors 13 (2023) 432, https://doi.org/10.3390/bios13040432.
[56] A.C. Notides, Binding affinity and specificity of the estrogen receptor of the rat uterus and anterior pituitary, Endocrinology 87 (1970) 987–992, https://doi.org/10.1210/endo-87-5-987.
[57] L.M. Hernandez, N. Yousefi, N. Tufenkji, Are there nanoplastics in your personal care products? Environ. Sci. Technol. Lett. 4 (2017) 280–285, https://doi.org/10.1021/acs.estlett.7b00187.
[58] N. Cennamo, D. Massarotti, L. Conte, L. Zeni, Low cost sensors based on SPR in a plastic optical fiber for biosensor implementation, Sensors 11 (2011) 11752–11760, https://doi.org/10.3390/s111211752.
[59] D. Materić, H.A. Kjær, P. Vallelonga, J.-L. Tison, T. Röckmann, R. Holzinger, Nanoplastics measurements in northern and southern polar ice, Environ. Res. 208 (2022), 112741, https://doi.org/10.1016/j.envres.2022.112741.
[60] D. Materić, R. Holzinger, H. Niemann, Nanoplastics and ultrafine microplastic in the Dutch Wadden Sea – the hidden plastics debris? Sci. Total Environ. 846 (2022), 157371 https://doi.org/10.1016/j.scitotenv.2022.157371.
[61] N. Cennamo, A.M. Bossi, F. Arcadio, D. Maniglio, L. Zeni, On the effect of soft molecularly imprinted nanoparticles receptors combined to Nanoplasmonic probes for biomedical applications, Front. Bioeng. Biotechnol. 9 (2021), https://doi.org/10.3389/fbioe.2021.801489.
[62] N. Cennamo, A. Piccirillo, D. Bencivenga, F. Arcadio, M. Annunziata, F. Della Ragione, L. Guida, L. Zeni, A. Borriello, Towards a point-of-care test to cover atto-femto and pico-nano molar concentration ranges in interleukin 6 detection exploiting PMMA-based plasmonic biosensor chips, Talanta 256 (2023), 124284, https://doi.org/10.1016/j.talanta.2023.124284.
[63] M. Thompson, S.L. Ellison, R. Wood, Harmonized guidelines for single-laboratory validation of methods of analysis (IUPAC Technical Report), Pure Appl. Chem. 74 (2002) 835–855, https://doi.org/10.1351/pac200274050835.
[64] J. Caldwell, P. Taladriz-Blanco, B. Rothen-Rutishauser, A. Petri-Fink, Detection of sub-micro- and nanoplastic particles on gold nanoparticle-based substrates through surface-enhanced Raman scattering (SERS) spectroscopy, Nanomaterials 11 (2021) 1149, https://doi.org/10.3390/nano11051149.
[65] C. Schwaferts, V. Sogne, R. Welz, F. Meier, T. Klein, R. Niessner, M. Elsner, N. P. Ivleva, Nanoplastic analysis by online coupling of Raman microscopy and field-flow fractionation enabled by optical tweezers, Anal. Chem. 92 (2020) 5813–5820, https://doi.org/10.1021/acs.analchem.9b05336.
[66] S. Oh, H. Hur, Y. Kim, S. Shin, H. Woo, J. Choi, H. H Lee, Peptide specific nanoplastic detection based on sandwich typed localized surface plasmon resonance, Nanomaterials 11 (2021) 2887, https://doi.org/10.3390/nano11112887.
[67] J. Li, G. Wang, X. Gou, J. Xiang, Q. ting Huang, G. Liu, Revealing trace nanoplastics in food packages—an electrochemical approach facilitated by synergistic attraction of electrostatics and Hydrophobicity, Anal. Chem. 94 (2022) 12657–12663, https://doi.org/10.1021/acs.analchem.2c01703.
[68] A.J. Kokalj, N.B. Hartmann, D. Drobne, A. Potthoff, D. Kühnel, Quality of nanoplastics and microplastics ecotoxicity studies: refining quality criteria for nanomaterial studies, J. Hazard Mater. 415 (2021), 125751, https://doi.org/10.1016/j.jhazmat.2021.125751.